Layer Formation in Stratified Taylor–Couette Flow

J. L. Partridge[1], C. Leclercq[2], C. P. Caulfield[1,3] and S. B. Dalziel[1]

[1]Department of Applied Mathematics and Theoretical Physics,
University of Cambridge
[2]School of Mathematics, Bristol University
[3]BP Institute, University of Cambridge
jlp56@cam.ac.uk

Abstract

A new set of high Reynolds number experiments ($Re = \frac{r_i \Omega_i \Delta r}{\nu} \sim 10^3 - 10^4$) are conducted to examine the layer formation observed in stratified Taylor–Couette flow. A wider range of radius ratios $\eta = \frac{r_i}{r_o}$ (where r_i and r_o are the radii of the inner and outer cylinder, respectively) than previously possible is explored to examine the universality of the dependence of layer height l on $\frac{U}{N}$, where U is a characteristic velocity scale and N is the buoyancy frequency. Previous work by Oglethorpe et al. (2013) found a linear relationship between l and $\frac{U}{N}$ taking a horizontal velocity scale $U_h = \sqrt{r_i \Delta r} \Omega_i$, where $\Delta r = r_o - r_i$ is the gap width and Ω_i is the rotation rate of the inner cylinder, and this choice of velocity scale is tested with our new, more comprehensive data set. The sensitivity of this scaling to initial conditions is also considered with the use of different spin up protocols, i.e. initiating the experiment in different ways. The different protocols include linearly increasing Ω_i with time to some final value, as well as initiating the experiment with a slow spin up, slow compared to viscous diffusion, to solid body rotation before impulsively stopping the outer cylinder.

1 Introduction

Spontaneous layer formation from an initial linear stratification within turbulent flows is not uncommon and layering within the ocean has been observed (for example, see figure 10.1 of Turner, 1979). There have also been a number of experimental studies investigating layer formation in stratified flows. Ruddick et al. (1989) and Park et al. (1994) observed layer formation when a vertical rod was towed through a stratified fluid, and a similar layering process was found by Holford and Linden (1999) when an array of vertical bars was used to drive the flow. Layering has also been observed experimentally in stratified Taylor–Couette flow by Boubnov et al. (1995) and Oglethorpe et al. (2013). However, the precise mechanism for the formation of the layers in high Schmidt number experiments at high Reynolds number is still not known and is crucial to the understanding of subsequent mixing within such flows as any buoyancy flux through the system ultimately has to pass over the highly stratified interfaces. We investigate the robustness of the layer formation mechanism here, by varying the initial conditions of the experiment, and propose a new scaling for the height of the layers.

The layout of the paper is as follows: §2 describes the experimental set-up followed by experimental observations in §3. Results are presented in §4 before concluding in §5.

2 Experimental Set-up

A pair of computer-controlled peristaltic pumps is used to fill the annulus between two concentric cylinders of radii r_i and r_o, for the inner and outer cylinder, respectively. Three inner cylinders with $r_i = \{6,\ 10,\ 15\}$ cm and two outer cylinders with $r_o = \{17,\ 24\}$ cm were used. One pump is connected to a reservoir containing relatively light fluid of density ρ_1 whilst the other is connected to a reservoir of denser fluid of density ρ_2. The two reservoirs of fluid are left for at least 24 hours to allow air to come out of the solutions (to minimise bubble formation during the experiment) and to let the solutions reach the ambient temperature of the laboratory. To fill the tank with a linear density stratification, the output of the two pumps is connected to a long, thin rod with a sponge outlet to minimise mixing, and the annulus region slowly filled from the bottom with increasing density solution. This technique has advantages over the double-bucket method as any stable density stratification can be achieved. However, for the present study we will only consider experiments that start with an initial linear stratification (ILS).

The inner cylinder was connected via a shaft to a brushless DC motor mounted overhead which was also computer controlled. This allowed the inner cylinder to be rotated over a range of angular velocities $0.1\ \mathrm{rads{\cdot}s^{-1}} < \Omega_i \leq 3\ \mathrm{rads{\cdot}s^{-1}}$ and the outer cylinder was attached to a turntable that could also rotate with a range angular velocities $0.1\mathrm{rads{\cdot}s^{-1}} < \Omega_o \leq 3.4\,\mathrm{rads{\cdot}s^{-1}}$ both with an error of $< 1\%$. The computer control allowed experiments to be initiated in different ways using different ramp protocols of the rotation rate Ω_i, i.e. varying the length of time taken to reach the maximum rotation rate. Experiments were initiated in three distinct ways with the ILS: impulsive start; linear ramp; and solid body rotation ramp. The impulsive starts experiments began by rotating the inner cylinder at Ω_i, with a short ($\leq T_{rot} = \frac{2\pi}{\Omega_i}$) ramp. Experiments with a linear ramp used a time dependent rotation rate $\hat{\Omega}_i$ of the form

$$\hat{\Omega}_i(t) = \begin{cases} \left(\frac{t}{T_{ramp}}\right)\Omega_i & t \leq T_{ramp} \\ \Omega_i & t > T_{ramp}, \end{cases} \tag{1}$$

where T_{ramp} is the time taken to reach the maximum rotation rate Ω_i from rest. Solid body rotation ramp experiments began by spinning up the annulus region to solid body rotation over a viscous time scale $T_\nu = \frac{\Delta r^2}{\nu}$ where Δr is the gap between the cylinders, i.e. $\Delta r = r_o - r_i$, and ν is the kinematic viscosity of the solution. When the ramp was finished the outer cylinder ceased to rotate, hence, at long times, the situation is identical to all other experiments, i.e. just the inner cylinder rotating. Explicitly,

$$\hat{\Omega}_i(t) = \begin{cases} \left(\frac{t}{T_\nu}\right)\Omega_i & t \leq T_\nu \\ \Omega_i & t > T_\nu \end{cases} \tag{2}$$

and

$$\hat{\Omega}_o(t) = \begin{cases} \left(\frac{t}{T_\nu}\right)\Omega_o & t \leq T_\nu \\ 0 & t > T_\nu. \end{cases} \tag{3}$$

For all experiments, the inner cylinder was painted matt white which allowed shadowgraph visualisation to be recorded. To this end, the experiment was illuminated from some distance ($\sim 2 - 3$ m) by a slide projector. This technique projects variation of the refractive index of the fluid in the annulus, highlighting regions of the flow that have

varying second derivatives of density, i.e. density interfaces. The projected pattern that formed on the inner cylinder was digitally recorded with a camera that had a small angular offset from the slide projector illuminating the flow. Alongside the visualisation, density profiles were measured throughout a large portion ($> 80\%$) of the height H of the experiment using a conductivity probe. The probe could take measurements at relatively high speed, traversing its full height (~ 35 cm) in approximately 3 s which is less than a rotation period T_{rot} for all of the experiments presented here.

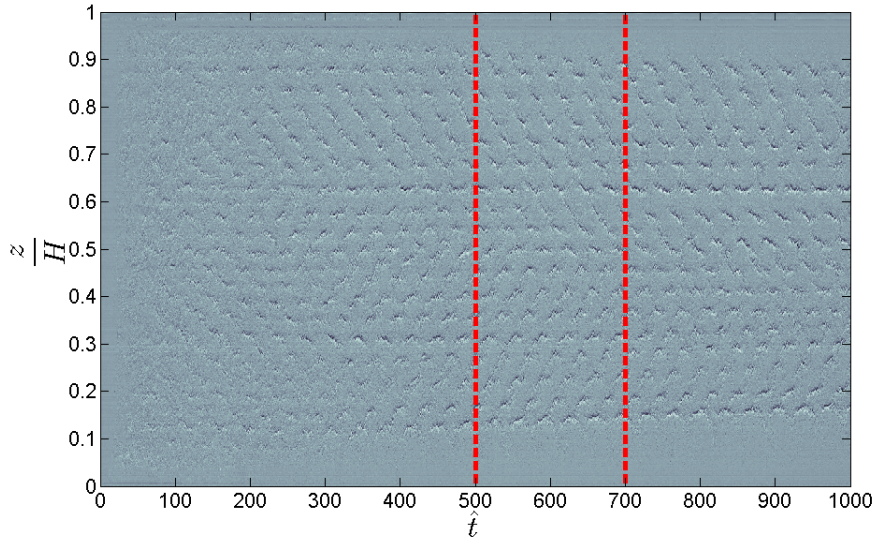

Figure 1: Time series of a shadowgraph visualisation from an impulsive start experiment. Regions of high contrast show the locations of sharp density interfaces. A clear periodic flashing of the interfaces is observed. The red dashed lines indicate the time window averaged in the analysis.

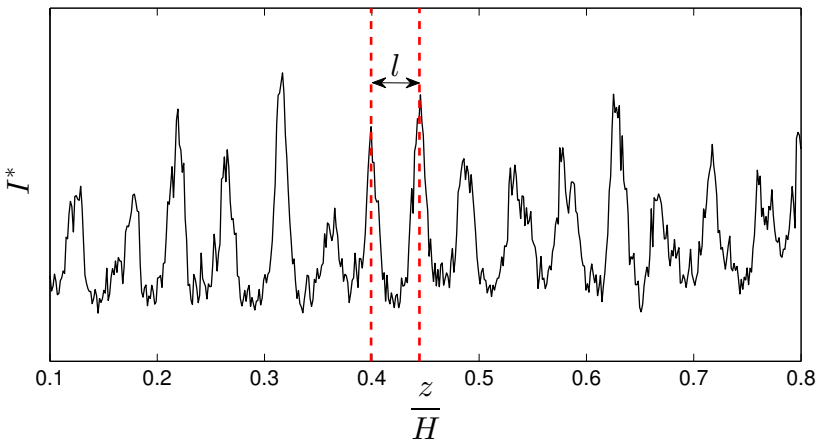

Figure 2: Intensity signal of the time-averaged shadowgraph time series. I^* is a measure of the light intensity. The red dashed lines, and double headed arrow, indicate the layer depth l extracted from the data.

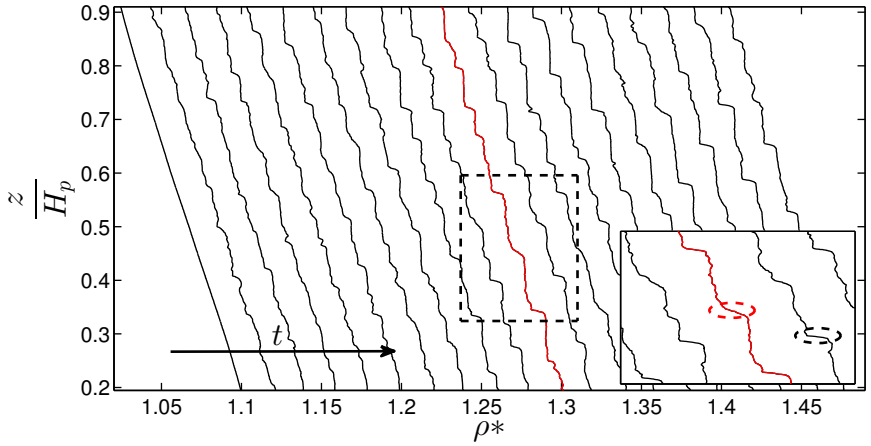

Figure 3: Evolution of density profiles with time for an experiment with $Re = 8750$, $N^2 = 3.08$, $r_i = 10$ cm and $r_o = 17$ cm. The time separation between profiles is $\Delta\hat{t} = 50.8$. The x-axis shows density ρ^* (g·cm^{-3}) with an arbitrary spacing of 0.02 between profiles to aid visualisation. The y-scale is vertical distance normalised with the depth of the probe measurement H_p (here 35 cm). The red line indicates the profile at $\hat{t} = 510$ and the box indicates the region of the inset. The inset shows a zoomed view of the profiles and highlights regions of high gradient, i.e. the location of a density interface.

3 Observations

For impulsive start experiments, turbulent motion can be seen within a few rotation periods of the inner cylinder. Rapidly, within 100-200 convective time units $\hat{t} = \left(\frac{r_i\Omega_i}{\Delta r}\right) t$, the motion appears to become organised in a banded structure, this is evident from the time series of the shadowgraph visualisation shown in figure 1. There is then a transient period, where these bands have some degree of tilt, before finally settling down to a quasi-steady period that appears to be linked to the formation of well-mixed layers.

The evolution of the density profiles during an experiment is shown in figure 3. With our new, high speed density profiles we are able to see the intermittent nature of the density interfaces, where an event is able to periodically mix the density interface. The periodic nature of this event is striking when observed on the time series of the shadowgraph as shown in figure 1 and appears to be similar to the periodic mixing event observed in two-layer stratified Taylor–Couette flow by Oglethorpe (2014). The periodic structure is currently under investigation in the ILS experiments but is not the focus of this paper.

The experiments with a linear ramp of the inner cylinder rotation rate show similar behaviour. However, experiments started by initially spinning up to solid body rotation have a lot more turbulent motion when the outer cylinder is stopped, due to the intense shear at this point, as is evident by the time series shown in figure 4. Nevertheless, the flow is still able to organise itself in to the same, preferred layered pattern. We now investigate quantitatively if the layer height is sensitive to the initialisation of the experiment and compare our results with a new scaling for the layer height l.

4 Results

To calculate the layer height of each experiment we make use of the shadowgraph visualisation. To compute the layer height we take a 200 convective time unit window from the

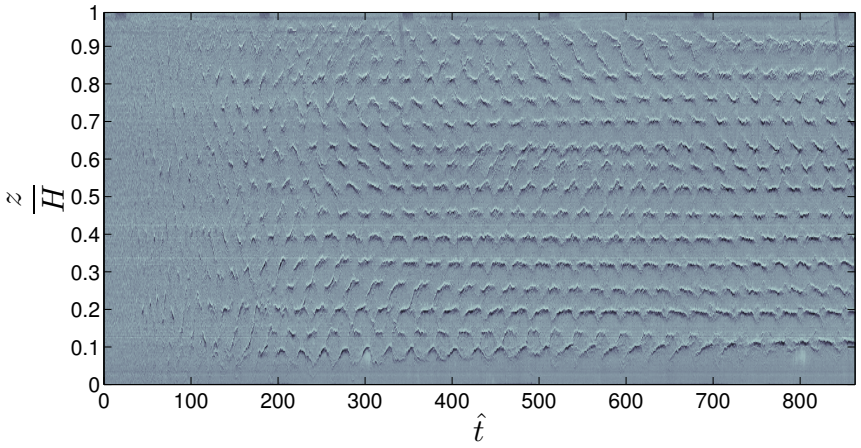

Figure 4: Time series of a shadowgraph visualisation from an experiment that started in solid body rotation.

time series (such as the one shown in figure 1) starting from $\hat{t} = 500$ to be sure we are in the quasi-steady regime. We then take the horizontal average of the image to effectively azimuthally average the features, hence removing the signature of the periodic event. The resulting waveform (the middle 3/5 of the flow field is analysed to remove end effects) is shown in figure 2 and shows a clear, periodic signal with wavelength representative of the layer height. This wavelength is extracted from the data with the use of the Fourier transform.

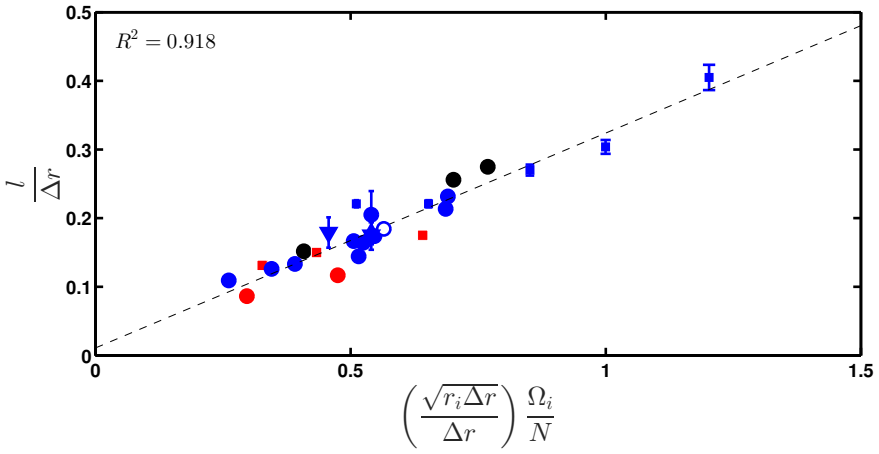

Figure 5: A comparison of the layer height found from all experiments with the scaling proposed by Oglethorpe et al. (2013) $\frac{\sqrt{r_i \Delta r}\Omega_i}{N}$ normalised by the gap Δr. The colour coding defines the inner cylinder radius, i.e. red ($r_i = 6$ cm), blue ($r_i = 10$ cm) and black ($r_i = 15$ cm), with symbols defining the outer cylinder radius, filled $\bigcirc$ ($r_o = 24$ cm) and filled $\square$ ($r_o = 17$ cm). Ramps are also represented as symbols with $\triangle$ ($T_{ramp} = 30$ min), $\triangledown$ ($T_{ramp} = 60$ min) and open $\bigcirc$ (solid body ramp). The dashed line shows the linear best fit to all the data with corresponding $R^2 = 0.918$.

Building on the work of Oglethorpe et al. (2013), a length scale can be formed from $\frac{U}{N}$ with a choice in the velocity scale U taken. Oglethorpe et al. (2013), following an argument of Boubnov et al. (1995), chose to use a horizontal velocity scale $U_h = \sqrt{r_i \Delta r}\Omega_i$ that collapsed their data well over a range of $\frac{\Omega_i}{N}$ and three different inner cylinders of

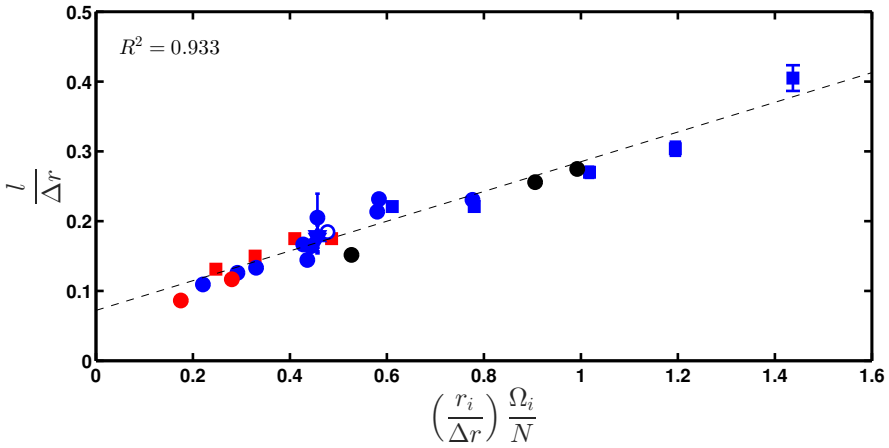

Figure 6: A comparison of the layer height found from all experiments with the proposed new scaling $\frac{r_i\Omega_i}{N}$ normalised by the gap Δr. The colour coding defines the inner cylinder radius, i.e. red ($r_i = 6$ cm), blue ($r_i = 10$ cm) and black ($r_i = 15$ cm), with symbols defining the outer cylinder radius, filled ○ ($r_o = 24$ cm) and filled □ ($r_o = 17$ cm). Ramps are also represented as symbols with △ ($T_{ramp} = 30$ min), ▽ ($T_{ramp} = 60$ min) and open ○ (solid body ramp). The dashed line shows the linear best fit to all the data with corresponding $R^2 = 0.933$.

varying r_i. However, the use of a fixed outer cylinder results in only a small change in the pre-factor of U_h as r_i and Δr are not changed independently. With our new dataset we propose a new choice of velocity scale in the layer depth scaling of the form $U = r_i\Omega_i$, i.e. the azimuthal speed at the inner cylinder.

Results across all experiments are shown in figures 5 and 6. Figure 5 shows the scaling proposed by Oglethorpe et al. (2013) and figure 6 shows the new scaling presented here. The new scaling appears to show better agreement to the data with a slightly higher R^2 value. This choice of scaling is counter-intuitive as it does not depend on the gap width Δr and suggests that the scale seen in the experiments is formed within the boundary layer at the inner cylinder. With the present dataset, it is hard to ascertain which scaling is most appropriate.

5 Conclusions

We have carried out a range of experiments in ILS Taylor–Couette flow to test the layer height scaling proposed by Oglethorpe et al. (2013) and also the sensitivity of the scaling to the initial conditions of the experiment. The formation of layers within the experiments appears to be robust to different initial conditions, with the same layer height found across a variety of different starting protocols.

We have proposed a new scaling for the layer height observed in stratified Taylor–Couette flow. The new scaling does not have a dependence on the gap width Δr which suggests that the scaling observed in the experiments is formed within the boundary layer at the inner cylinder. Further experiments will be carried out to vary the radius ratio η to see if the layer height scaling breaks down for small ($\eta \sim 1$) and large ($\eta \sim 0$) gaps along with simultaneous particle image velocimetry (PIV) and light induced fluorescence (LIF) to shed light on the layer formation mechanism.

Acknowledgements

The authors would like to acknowledge the Mathematical Underpinnings of Stratified Turbulence EPSRC Programme Grant (EP/K034529/1) for funding this research and thank the technical staff of the G. K. Batchelor Laboratory for their assistance.

References

Boubnov, B. M., Gledzer, E. B., and Hopfinger, E. J. (1995). Stratified circular couette flow: instability and flow regimes. *J. Fluid Mech.*, 292:333–358.

Holford, J. M. and Linden, P. F. (1999). Turbulent mixing in a stratified fluid. *Dynamics of Atmospheres and Oceans*, 30(2):173–198.

Oglethorpe, R. L. F. (2014). *Mixing in stably stratified turbulent Taylor-Couette flow*. PhD thesis, University of Cambridge.

Oglethorpe, R. L. F., Caulfield, C. P., and Woods, A. W. (2013). Spontaneous layering in stratified turbulent taylorcouette flow. *J. Fluid Mech.*, 721:R3 (12 pages).

Park, Y., Whitehead, J. A., and Gnanadeskian, A. (1994). Turbulent mixing in stratified fluids: layer formation and energetics. *J. Fluid Mech.*, 279:279–311.

Ruddick, B., McDougall, T., and Turner, J. (1989). The formation of layers in a uniformly stirred density gradient. *Deep Sea Research Part A. Oceanographic Research Papers*, 36(4):597–609.

Turner, J. S. (1979). *Buoyancy effects in fluids*. Cambridge University Press.